RSC Advances

ROYAL SOCIETY OF CHEMISTRY

www.rsc.org/advances

Synthesis, characterization and properties of a bio-based elastomer: Polymyrcene

Preetom Sarkar, Anil K. Bhowmick*

Table of Contents

Bio-based elastomer from renewable resources

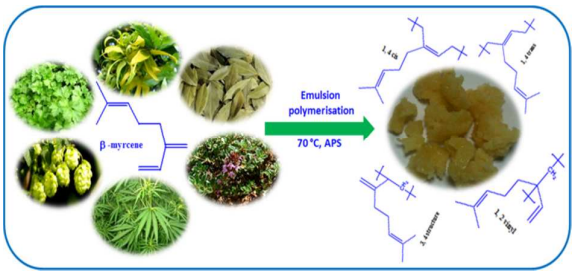

Cite this: DOI: 10.1039/c0xx00000x

www.rsc.org/xxxxxx

PAPER

Synthesis, characterization and properties of a bio-based elastomer: Polymyrcene

Preetom Sarkar[a], Anil K. Bhowmick[*b]

Received (in XXX, XXX) Xth XXXXXXXXX 20XX, Accepted Xth XXXXXXXXX 20XX

DOI: 10.1039/b000000x

Environmentally benign emulsion polymerisation technique was exploited to prepare a bio based polymer from naturally occurring monoterpene, β-myrcene. The structure of the polymer was ascertained by spectroscopic measurements. Density functional theory was employed to determine the ground state optimised structure of β-myrcene. The persulfate initiated polymyrcene possesses *3, 4* and *1, 2 vinyl* defects along with *1, 4* microstructures, whereas the redox analogue contains solely *1, 4* addition products. The synthesised polymer displayed substantially high molecular weight (up to 92,860 Da for persulfate polymyrcene) and subzero (-73 °C) glass transition temperature along with shear thinning behaviour within the experimental conditions, thereby rendering itself as a promising entrant in the domain of bio-based elastomer.

Keywords: Emulsion polymerisation, β-myrcene, Density functional theory, Bio-based elastomer, Rubber

Notes:

[a]*Department of Chemistry, School of Basic Science, Indian Institute of Technology Patna, Patna - 800013, India*

[b]*Rubber Technology Centre, Indian Institute of Technology Kharagpur, Kharagpur - 721302, India. Email: anilkb@rtc.iitkgp.ernet.in, anilbhowmick@gmail.com, Tel.: +91 (3222) 283180; Fax: +91 (3222) 220312*

†Electronic Supplementary Information (ESI) available: [Wide angle XRD analysis, Particle morphology of the latex emulsion]

Introduction

The outbreak of synthetic elastomer technology and elastomer as a strategic material is well documented in the history of World War II. The basic building blocks of synthetic elastomer are either derived from petrochemical resources (fossil fuel) or part of it contains petro-based synthons. As these resources dwindle with time, along with its price volatility and environmental ill effects, the scientific community is in dire search for a suitable replacement of the current petro based elastomers by sustainable alternatives. [1] This paradigm shift of surge is reflected in the announcement of Genencor and Amyris company to launch BioIsoprene® as a replacement for its petro based analogue. [2, 3] Thus, it is evident that the impetus for growth in this domain will surely rely on the development of environmentally benign methodologies which utilise abundant bio-resources.

Nature produces rubber latex in over two thousand plant species by bio-synthetic (isopentenyl pyrophosphate) route. [4] On the other hand, terpenes or terpenoids refer to one of the largest families of naturally occurring compounds and are secondary metabolites synthesized mainly by plants, particularly conifers. [5, 6] Though most terpenes share isoprene (2-methyl-1, 4-butadiene) as an elementary unit ('isoprene rule') [7], nature does not produce any polymer out of it. Thus, due to their abundance in nature, there has been great interest in producing polymers with terpenes as either functional entities or as the main constituent. [8] To make use of the chemical functionalities (unsaturation, functional groups) present in terpene molecules, various chemical strategies and a wide range of polymerisation techniques [9 – 19] had been studied. Unlike the terpenes used in the aforementioned reports, the acyclic monoterpene: 7-methyl-3-methylene-1, 6-octadiene or β-myrcene resembles the classical chemistry of other petro based unsaturated hydrocarbons. β-myrcene is a component of essential oil of various plants like wild thyme, ylang-ylang, bay, cannabis, parsley, hops and its use as a fragrance and flavours are known from antiquity. [20] Commercially, β-myrcene is prepared from the pyrolysis of β-pinene. Its use as a potential diesel fuel additive after hydrogenation is also reported in literature. [21] Interestingly, very little thrust has been given to exploit this natural product in the field of elastomer and tyre technology. Kobayashi *et al.*[22] prepared poly(3-methylenecyclopentene) using a combination of ring-closing metathesis and cationic polymerization starting from myrcene. Loughmari *et al.* [23] reported co-ordination polymerisation of β-myrcene. Marval and Hwa [24] studied the polymerisation of myrcene using Ziegler-type catalyst. Recently, Choi and Ritter [25] reported a free radical copolymerisation of myrcene with diethyl fumarate and styrene, utilising water soluble β-cyclodextrin complex. All of the methodologies mentioned essentially rely on either utilisation of volatile organic compounds (especially solvents) or specialised techniques (catalyst), and were not carried out with application in mind. Thus, despite some studies on terpene-based polymers, the increasing leap for environmentally benign methodologies demands further development and implementation of a green polymerisation technique in this domain which will supplement the dearth of bio based synthetic elastomer. Being a solvent less and mature system along with its multitude of advantages (faster rate, high molecular weight products), emulsion polymerisation [26, 27] is cynosure in this area.

With our quest to develop a bio-based elastomer by employing a green technique, we herein report the persulfate as well as redox initiated emulsion polymerisation of β-myrcene and intend to give an insight into the chemical structure and the properties of the synthesised polymer. Vulcanisate properties of polymyrcene was first reported by Johanson *et al.* [28], although there was no work on the structure or characterisation or optimisation of the experimental conditions to obtain the best properties of the pristine polymer. Surprisingly, this polymer did not find attention for a long time after the preliminary investigation. We feel that further studies should be

done to exploit its commercial viability in view of recent focus on sustainable and green elastomer. To the best of our knowledge, this is the first report of its kind which presents an in-depth analysis of the microstructure of the as obtained polymer using environmentally benign emulsion polymerisation technology along with theoretical calculation and elucidation of properties. The optimised structure of β-myrcene was determined using Density Functional Theory (DFT) calculation. The reactivity of the molecule was ascertained with the help of frontier molecular orbital theory and electrostatic potential (ESP) mapping. Thermal stability, various transitions and mechanical and dynamic mechanical properties of the synthesised polymer were measured and the findings were correlated with the microstructure. Furthermore, the particle nature of the emulsion latex was also reported.

Experimental

Materials

β-myrcene (99%) was purchased from Sigma Aldrich company and the inhibitor, butylated hydroxytoluene was removed by shaking with 2(M) NaOH solution. Sodium dodecyl sulphate (SDS, 99%) was procured from Loba Chemie, India and used as received. Ammonium persulphate (APS, 98%) and sodium bicarbonate ($NaHCO_3$, 99%) were obtained from E. Merck (India). Ferrous sulphate heptahydrate ($FeSO_4.7H_2O$, 98%) was purchased from Alfa Aesar India. Ethylenediaminetetraacetic acid sodium salt, Potassium oleate, potassium phosphate tribasic (K_3O_4P), potassium chloride (KCl), sodium hydroxymethane sulfinate (SHS) and *tert*-butyl hydroperoxide solution (Luperox® TBH70X), were purchased from Sigma Aldrich company and used without further purification. All other chemicals were reagent-grade commercial products and used as received without further purification. Deionised water (DI) was taken for all the experiments.

Persulfate initiated emulsion polymerisation of β-myrcene

Persulfate initiated emulsion polymerisation of β-myrcene was carried out following the recipe mentioned in Table 1. The general procedure followed for the emulsion polymerisation was as follows: At first, the emulsifier (SDS), DI water and buffer ($NaHCO_3$)

Table 1: Recipe for persulfate-initiated emulsion polymerization

Ingredients	Amount (g, in phr*)
Monomer	100
DI water	250
Sodium dodecyl sulphate (SDS)	2.5
Ammonium persulfate (APS)	0.35
Sodium bicarbonate ($NaHCO_3$)	1.5

**parts per hundred parts of rubber*

were added into the round bottom flask and mixed thoroughly at 250 rpm for 20 min to form the micelle. Thereafter, the β-myrcene monomer was added slowly over a period of 10 min and left as such for a further 20 min so as to obtain a stable emulsion. Then, the reactor was flushed twice with nitrogen and the temperature was set to 70 °C. Aqueous solution of the initiator (APS) was added into the reaction mixture drop-wise over 20 min in two intervals. The reaction was continued for 20 hrs to obtain a stable latex. Initially, the colour of the reaction mixture was off white, but with the progress of the reaction a light blue tinge appeared due to the particle growth in the emulsion medium (Tyndall effect). After the stipulated time, the latex was coagulated using excess acidified ethanol with continuous stirring. The obtained polymyrcene (PMy) was taken out, washed profusely with DI water to remove the traces of emulsifier and

subsequently dried at 50 °C in vacuum for 24 hrs. The polymerisation is shown in Scheme 1. Polymerisation was also carried out at different temperatures (60 - 80 °C) and different times (4 – 24 h).

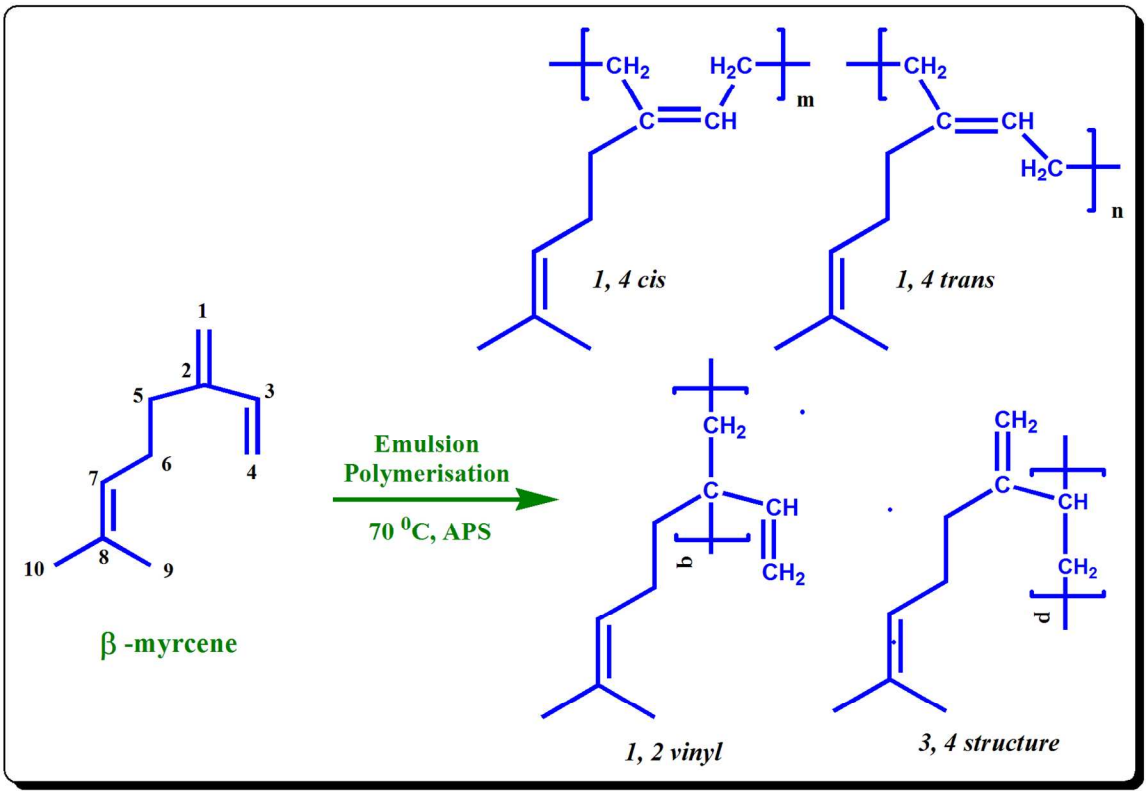

Scheme 1: Emulsion polymerisation of β-myrcene

Redox initiated emulsion polymerisation of β-myrcene

According to the recipe furnished in Table 2, redox initiated emulsion polymerisation was performed following strict addition sequence. At first, DI water, potassium oleate, potassium chloride and potassium phosphate tribasic buffer were charged into a round bottom flask and stirred at 250 rpm for 20 min. Subsequently, β-myrcene was introduced into the flask and mixed thoroughly for a further 20 min. Upon obtaining a stable emulsion, SHS, $FeSO_4$ and Na-EDTA were added to the mixture. Thereafter, the reactor was flushed with nitrogen to remove traces of air, followed by the injection of TBHP solution into the flask. The polymerisation was allowed to proceed for 20 hrs at 25 °C. The obtained latex was then coagulated using excess acidified ethanol. The as obtained polymer was washed profusely with DI water and dried in vacuum oven at 50 °C for 24 hrs.

Table 2: Recipe for redox-initiated emulsion polymerization

Ingredients	Amount (g, in phr*)
Monomer	100
DI water	180
Potassium oleate	4.5
Potassium chloride	0.3
Potassium phosphate tribasic	2.0
tert-butyl hydroperoxide solution (TBHP)	0.06
Ferrous sulphate heptahydrate ($FeSO_4$, $7H_2O$)	0.01
Ethylenediaminetetraacetic acid sodium salt	0.05
Sodium hydroxymethane sulfinate (SHS)	0.05

**parts per hundred parts of rubber*

Measurements and characterisation

Polymer molecular weight was determined by Agilent PL-GPC 50 instrument, using PLgel 5µm Mixed-D column equipped with a refractive index detector and tetrahydrofuran as the eluent (sample concentration 1mg/ml). The GPC data were recorded at 25 °C at a flow rate of 1ml/min (polystyrene standards were used for calibration). In order to determine the gel fraction of the synthesised polymers, the samples were extracted using THF under reflux condition for 8 hrs. The gel percentage was calculated as the ratio of dried polymer weight to its original value.

The FT-IR spectra were recorded in Universal Attenuated Total Reflectance mode (UATR) using Perkin Elmer Spectrum 400 machine in a spectral range of 4000–650 cm^{-1} with a total of 8 scans per sample (resolution 4 cm^{-1}).

^1H NMR and ^{13}C NMR spectrum were recorded in a AVANCE III 400 Ascend Bruker instrument operating at 400 MHz. $CDCl_3$ was used as a solvent and the chemical shift values were reported in δ (ppm) relative to the ^1H signals from the internal standard tetramethylsilane (TMS). The peak for deuterated solvent appeared at δ = 7.19 ppm for ^1H NMR and δ = 77.22 ppm for ^{13}C NMR.

Raman spectroscopy was recorded using an STR 750 series (Seki Technotron/ Technos Instrument India) Raman spectrometer with a 633nm He-Ne laser source and a grating of 600 lines per mm. The samples were placed on the sample stage and the laser focused on a

specific area of the samples using 50X objective lens of the attached microscope (Olympus BX-51). The results reported are an average of data collected over 5 different points.

Density functional theory (DFT) calculation was carried out using Gaussian-09 software. The geometry (optimised structure) and frequency of β-myrcene were calculated with Becke's three-parameter hybrid functional (B3LYP) method by using 6-311G (d, p) as basis set. The electrostatic potential map (ESP) density of the optimised structure was generated using ArgusLab 4.0.1 software.

Differential scanning calorimetry measurements were recorded in a Perkin Elmer DSC8000 under nitrogen atmosphere. The following heating protocol was followed: the sample was heated from -96 °C to +100 °C, equilibrating at +100 °C for 2 min, cooling from +100 °C to -96 °C, equilibrating at -96 °C for 2 min, reheating from -96 °C to +100 °C. The heating or cooling rates were 5 °C/min in all the cases. To eliminate the thermal history, transition temperature was reported from the second heating run. Thermogravimetric analysis were carried out using SDT Q600 (TA Instruments) under nitrogen flow at a ramp rate of 10 °C/min.

The dynamic mechanical properties of synthesised polymer were measured using a DMA-Q800 machine in tension mode. All the samples (11 × 6.3 × 0.24 mm) were analyzed at a constant frequency of 1 Hz, at a heating rate of 3° C/min and strain amplitude of 30 µm over a temperature range of -100 °C to +100 °C. Because of low strength of the synthesised polymer, the glass fibre cloth was impregnated with a solution of the polymer in chloroform and a thin film of uniform thickness was deposited on it followed by drying at room temperature. Glass fibre cloth was chosen as it did not show a glass transition within the temperature range of interest. [29] Only the Tan Delta peak was taken into account from this experiment.

The rheological measurements were performed using a MCR302 Anton Paar Modular Compact Rheometer having parallel plate geometry of 8 mm diameter and with a 1.1 mm gap in between the plates. Frequency sweep experiments were conducted at 30 °C and at a constant strain of 0.2% in the frequency range between 0.1 to 10 Hz. Temperature sweep experiments were carried out at 0.2% constant strain and 1Hz frequency in between -10 °C to +100 °C temperature employing a ramp rate of 3 °C/ min.

The stress-strain behaviour of the synthesised polymyrcene was recorded using Tinius Olsen H5KS UTM machine with a 5N load cell at room temperature and a cross-head speed of 25 mm/min. The samples for tensile testing were prepared by solution casting technique. As the samples were weak, attempt to prepare the dog-bone type tensile specimen by using standard ASTM (D412) cutter created wrinkles and defects in the samples. Hence, it was decided to prepare rectangular samples. [30] The dimensions of the rectangular tensile specimen were: length = 35mm, width = 7.5mm, thickness = 0.5mm.

Wide angle X-ray diffraction analysis was carried out using Rigaku TT RAX3 XRD machine in the range of 2θ from 10° - 50° (scan rate 3° per minute) with CuKα (0.154nm) as radiation source at 50kV and 100mA.

The morphology of the latex was characterised using field emission scanning electron microscope (Hitachi, S-4800 FESEM) at an accelerating voltage of 10kV. The latex was diluted with water and sonicated prior to casting and drying on silicon wafer and thereafter

coated with gold by using Hitachi E-1010 ion sputter system. The particle nature of the latex was analysed by dynamic light scattering (DLS) method using Delsa® Nano Submicron Particle Size and Zeta Potential Particle Analyzer PN A54412 from Beckman Coulter with a laser as a light source and a detector that detected the scattered light at an angle of 165°.

All the experimental results on characterisation and polymerisation were based on three measurements.

Results and discussion

Synthesis of Polymyrcene (PMy) by emulsion polymerisation

Ammonium persulfate initiated emulsion polymerisation of β-myrcene was performed at 70 °C at atmospheric pressure. High temperature was maintained to furnish sufficient free radicals for the polymerisation process. Sodium dodecyl sulphate (SDS) was used as a surfactant and sodium bicarbonate was used as a buffer. Based on the polymer molecular weight and percentage yield, the optimised reaction conditions (polymerisation time and reaction temperature) for persulfate initiated process were frozen, and all the analysis was carried out using the polymer synthesised at the optimised set of reaction conditions. To facilitate the polymerisation process at room temperature, redox emulsion technique was also carried out. Na-EDTA was used as a sequestering agent, sodium hydroxymethane sulfinate (SHS) was used as an oxidant, ferrous sulphate heptahydrate ($FeSO_4$, $7H_2O$) as a reductant and *tert*-butyl hydroperoxide (TBHP) as a free radical generator.

Time and Temperature dependence of PMy synthesis

In order to investigate the effect of time and temperature on the PMy synthesis, the persulfate initiated emulsion polymerisation was carried out at first at five different temperatures of 5 °C interval and for a fixed reaction time of 20 hrs. The lower and upper limit of the temperature is such chosen to ensure complete initiator decomposition in the former case (well above the half life temperature of the initiator species) and preventing destabilisation of the dispersion medium (i.e. water) of the polymerisation system respectively. Fig. 1a shows that with increasing temperature, both molecular weight and percentage yield exhibit increasing trend up to 70 °C, after which a reversion trend is followed. This can be attributed to the fact that with increase in temperature, the propagation rate of the reaction increases; but at high temperature, thermal decomposition of the polymer chains predominates, thereby reducing the molecular weight and percentage yield value. Thus, 70 °C was chosen as the optimum reaction temperature. To study the effect of time on the polymerisation reaction, aliquots were taken out from the reaction mixture at 4 hr. time interval and up to 24 hours followed by GPC measurements and yield calculation.

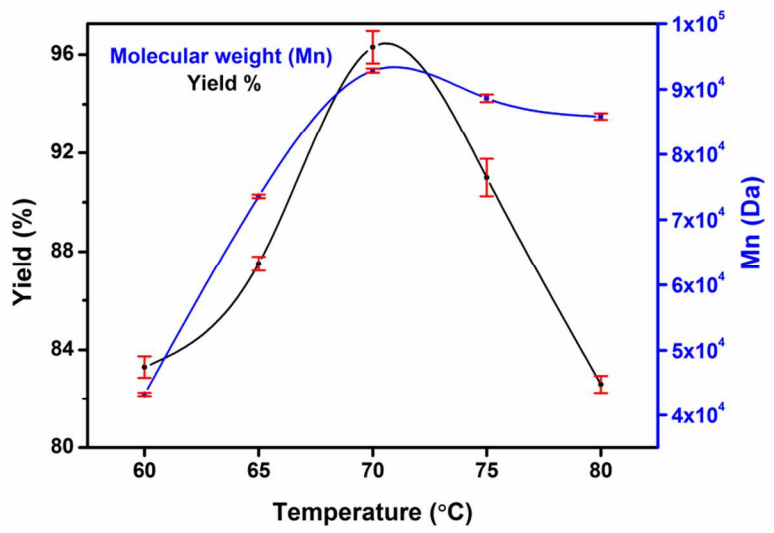

Fig. 1a: Temperature dependence of PMy synthesis on yield and molecular weight

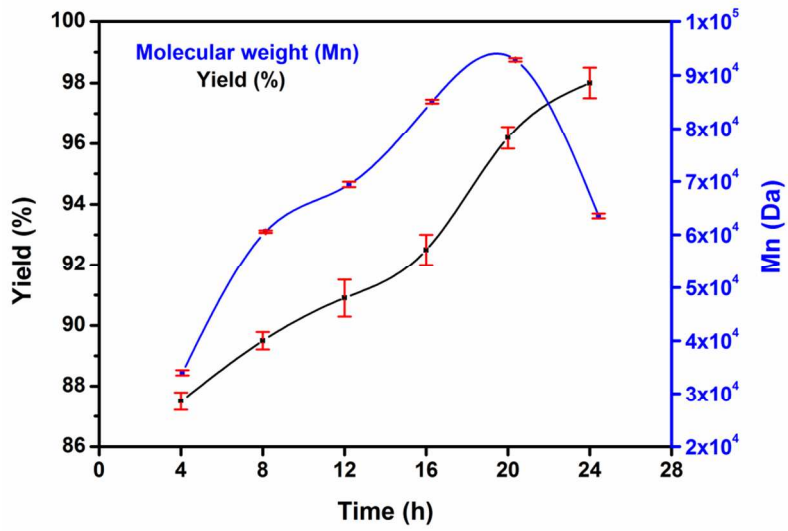

Fig. 1b: Time dependence of PMy synthesis on yield and molecular weight

It is evident from Fig. 1b that percentage yield increases with reaction time and the molecular weight reaches its maximum value of 92,860 Da at 20 hrs. In line with the temperature effect, at higher reaction time, chain scission occurs which produces oligomers and hence there is a decreasing trend of molecular weight at long reaction time. [27] Therefore, from the cumulative study of temperature and time dependence, the optimum reaction condition for the persulfate initiated emulsion polymerisation was fixed at 70 °C for 20 hrs. Table 3 summarises the molecular weight and yield values for the synthesised PMy at different conditions. Redox initiated polymerisation yields polymer with high molecular weight in comparison to persulfate initiated one (Table 3). This is because the redox reaction was carried out at room temperature, and the side reactions and chain transfer effects are suppressed which facilitate the

production of high molecular weight polymer. Due to micro crosslinking between the growing chains (two nos. of residual unsaturation in the polymer structure), the gel content of the synthesised polymer increases with increasing reaction temperature and time. For the redox system, the high gel content value is in good agreement with other studies. [25]

Table 3: Molecular weight and percent yield of persulfate and redox initiated PMy

Sample	Time (hrs.)	Temperature (°C)	Mn (Da)	PDI	% Gel	% Yield
$PMy_{60°C}$	20	60	43,270 (± 250) [#]	2.64	5	83.0 (± 0.4)
$PMy_{65°C}$	20	65	73,570 (± 280)	2.51	7	87.0 (± 0.3)
$PMy_{70°C}$	20	70	92,860 (± 300)	2.48	12	96.0 (± 0.6)
$PMy_{75°C}$	20	75	88,650 (± 590)	2.42	14	91.0 (± 0.8)
$PMy_{80°C}$	20	80	85,850 (± 490)	2.55	14	83.0 (± 0.4)
PMy_{4h}	4	70	33,970 (± 490)	1.77	2	87.0 (± 0.3)
PMy_{8h}	8	70	60,580 (± 220)	2.25	5	89.0 (± 0.3)
PMy_{12h}	12	70	69,450 (± 500)	2.27	8	91.0 (± 0.6)
PMy_{16h}	16	70	75,140 (± 380)	2.26	9	93.0 (± 0.5)
PMy_{20h}	20	70	92,860 (± 300)	2.48	12	96.0 (± 0.4)
PMy_{24h}	24	70	63,550 (± 450)	3.02	12	98.0 (± 0.5)
PMy_{redox}	20	25	1,09,780 (± 410)	3.13	17	66.0 (± 0.7)

[#]*Values in the parenthesis indicate the standard deviation based on three measurements.*

FT-IR and NMR characterisation of the synthesised PMy

Fig. 2 represents the FT-IR spectra of β-myrcene and PMy_{20h}. The weak peak at 3093 cm^{-1} in the monomer represents the =C-H stretching of C1, C3 and C4, which disappears upon polymerisation. The broad absorption peaks at 2970, 2931 and 2860 cm^{-1} in the monomer are assigned to the $–CH_3$, $-CH_2$ and –CH asymmetric stretching vibration respectively, which get broadened due to the formation of more number of such groups in the polymer. The strong absorption peak at 1596 cm^{-1} is assigned to C1=C2 and C3=C4 stretching frequency (Fig. 2). Due to conjugation, this stretching appears at lower wave number value. A small peak at 1641 cm^{-1} can be ascribed to the presence of isolated C7=C8 in the structure. The disappearance of the former C=C peaks and simultaneous broadening of the latter one indicates to the consumption of C1=C2 and C3=C4 during the polymerisation process followed by formation of C2=C3 and simultaneous retention of the isolated unsaturation. The confinement of C-H bending peak for tri substituted alkene (here C7) at 824 cm^{-1} even after polymerisation reiterates that the isolated double bond is indeed preserved during polymerisation (which is evident from

theoretical calculation discussed later). The characteristics absorption peaks around 1444 and 1376 cm^{-1} are due to the $–CH_2$ and $–CH_3$ bending vibration of C5-C6 and C9-C10 centres respectively. After polymerisation, generation of more methylene unit is reflected in the relative increment of the corresponding peak area at 1444 cm^{-1}. The strong absorption peaks around 992 and 889 cm^{-1} in the monomer is due to the sp^2 C-H bending vibration of C1, C3 and C4 centres respectively. While the sharp decrease in the intensities of these bands in the polymer is due to the consumption of these two unsaturations (C1=C2 and C3=C4) during polymerisation, the small residual peak in these two regions is due to the formation of *3, 4 structure* (C1=C2 is preserved) and *1, 2 vinyl* (C3=C4 is preserved) structure in the polymer as ascertained from the NMR analysis discussed in the next section. The small peak at 735 cm^{-1} is due to the $–CH_2$ rocking vibration which is preserved in the polymer with lower intensity due to restriction of rocking movement in the macromolecular chains.

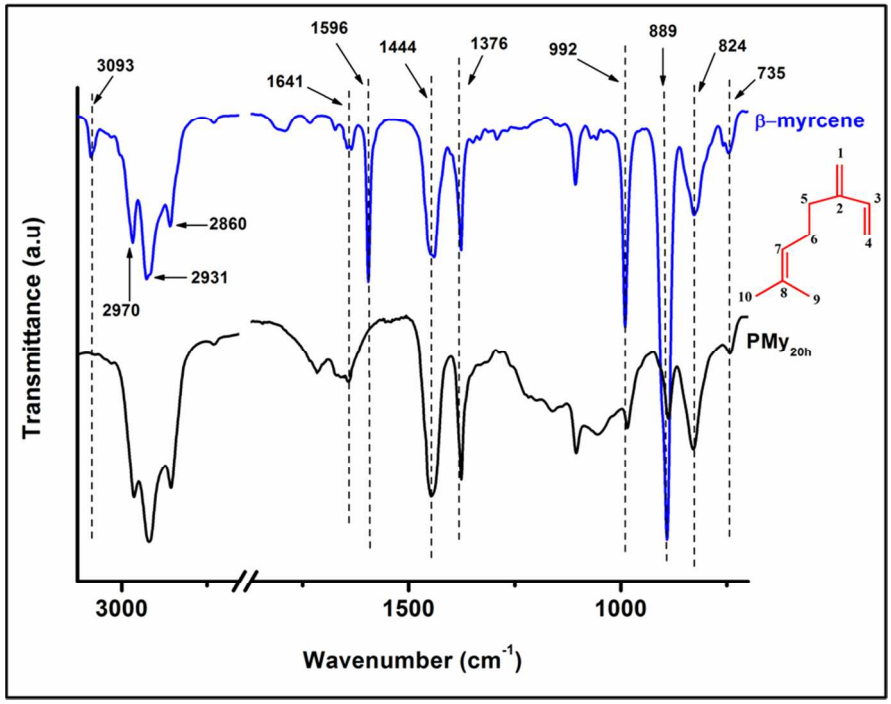

Fig. 2: FT-IR spectra of β-myrcene and PMy_{20h}

^1H and ^{13}C NMR characterisation of the synthesised PMy

The ^1H and ^{13}C NMR (inset) spectra of β-myrcene are presented in Fig. 3a. Fig. 3b-3c represents ^1H and ^{13}C NMR spectra of persulfate initiated polymyrcene (PMy_{20h}) respectively. The spectral signals are well assigned to various magnetically different protons and carbons. The structure of the monomer is much like an isoprene unit, except the methyl group is replaced by an aliphatic chain having an isolated unsaturation (i.e. C7=C8). Thus, the polymer may have four different types of microstructure viz. *1, 4 -cis, 1, 4 -trans, 1, 2 -vinyl* and *3, 4* polymyrcene. The spectral assignments are in good accord with the available literature. [23, 31] The sequencing of the carbon atoms are adopted from the literature. [23, 31]

^{1}H NMR data of PMy_{20h} ($CDCl_3$, 400 MHz, δ ppm): 5.32 [3''' H]; 5.04 [3, 7, 3', 7', 7'' and 7''' H]; 4.69 [4''' H]; 4.68 [1'' H]; 1.96 [1, 4, 5, 6, 1', 4', 5', 6', 3'', 4'', 5'', 6'', 1''', 5''', 6''' H]; 1.60 [10, 10', 10'', 10''' H]; 1.52 [9, 9', 9'', 9''' H]. (Please see figures for designation)

The protons of the two methyl groups attached to C8 in all the microstructures appear at upfield values (δ = 1.60 ppm and 1.52 ppm). The methylene protons of all the microstructures appear as a broad peak at 1.96 ppm. The upfield shift of all these protons relative to their monomer can be ascribed due to the generation of long chain macromolecules which shield each other from the external magnetic field (*cf*. Fig 3a and Fig. 3b).

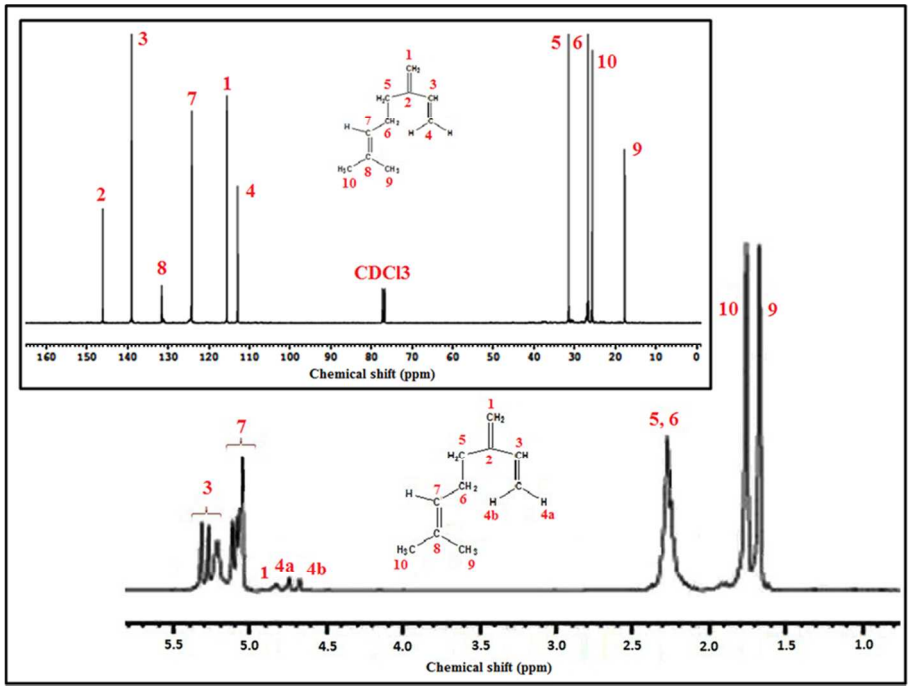

Fig. 3a: ^{1}H and ^{13}C NMR spectra of β-myrcene

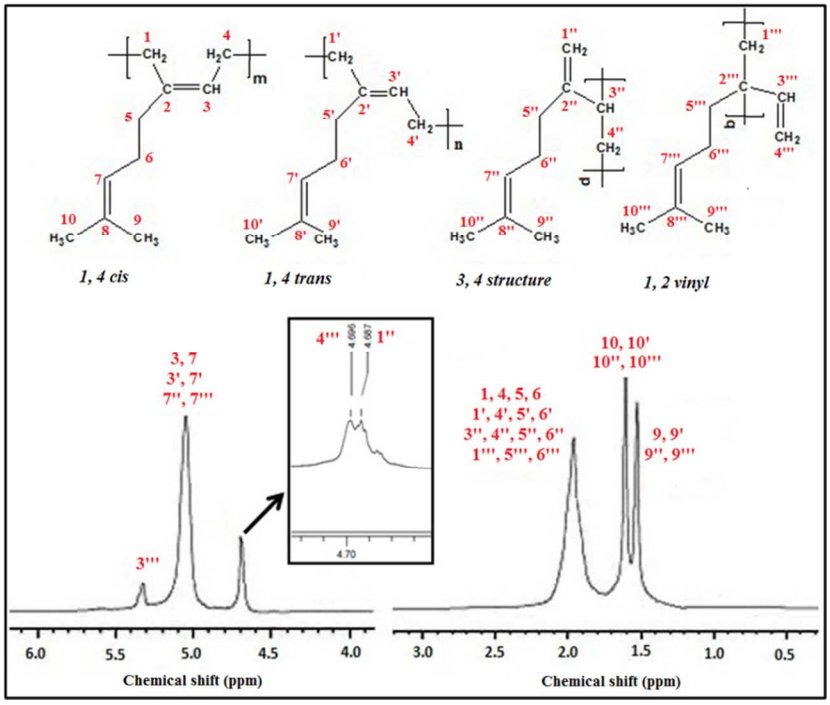

Fig. 3b: ^{1}H NMR spectrum of PMy_{20h}

According to the literature report [32, 33] available on NMR studies of polyisoprene, the peaks above 4.5 ppm indicates the olefinic protons of *1, 2 vinyl* addition (5.32 ppm of 3''' H). A close look into the peak around 4.6 ppm reveals the presence of two splitting pattern at 4.69 ppm (4''' H of *1, 2 vinyl*) and 4.68 ppm (1'' H of *3, 4 structure*). The olefinic =CH- for both *1,4 –cis, 1,4 –trans* as well as =CH- of C7 appears as a single peak at 5.04 ppm. Taking these three peaks (δ = 5.04, 4.69 and 4.68 ppm) into account, it is estimated that the persulfate initiated polymyrcene consists of 47 % *1,4 –cis* and *1,4 –trans* mixture, 29% *1, 2 vinyl* and 24% *3, 4 srtucture*. As no signature peak for *1, 4 –cis and 1, 4 –trans* structure was obtained, exact percentage of these microstructures could not be determined.

^{13}C NMR data of PMy_{20h} ($CDCl_3$, 400 MHz, δ ppm): 154.34 [2'' C]; 137.5 [2, 2' C]; 131.54 [8, 8', 8'', 8''' C]; 124.69 [3, 7, 3', 7', 7'', 3''', 7''' C]; 107.14 [1'', 4''' C]; 40.37 [2''' C] 39.97 [3'' C]; 37.86 [5 C]; 37.61 [5'' C]; 37.40 [5', 5''' C]; 29.71 [1' C]; 29.07 [1''' C]; 28.34 [1 C]; 27.98 [4', 4'' C]; 27.16 [4 C]; 27.01 [6, 6' C]; 26.84 [6'' C]; 26.51 [6''' C]; 25.86 [10, 10', 10'', 10''' C]; 17.71 [9, 9', 9'', 9''' C].

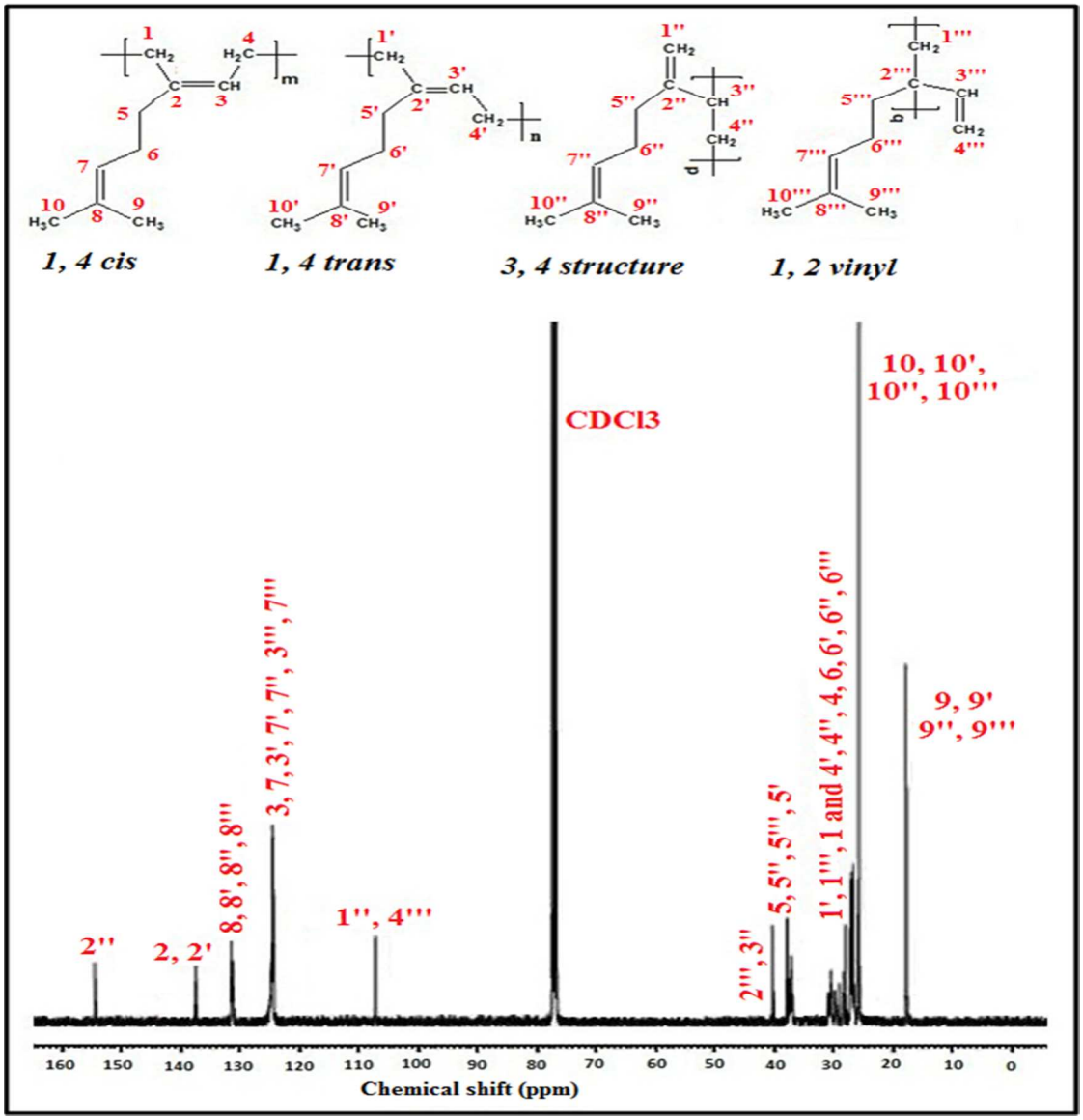

Fig. 3c: ^{13}C NMR spectrum of PMy_{20h}

The ^{13}C NMR spectrum of persulfate initiated PMy shows several sharp peaks and few overlapped peaks in the region of δ = 25 – 30 ppm. Due to long macromolecular chains, the exact degeneracy of the peaks in ^{13}C NMR spectra is very much unlikely. Peak at 154 ppm suggests the formation of *3,4 structure* in the polymer. 2C and 2'C in *–cis* and *–trans* structures respectively appear at lower ppm (δ = 137.5 ppm) , as they are part of the main chain of the polymer. The retention of peaks around 131.5 and 124.6 ppm in polymer (131.5 and 124.2 ppm respectively in monomer) indicates that the isolated unsaturation (C7=C8) is indeed preserved and polymerisation took place at C1=C2 and C3=C4 position. The peak for 3C, 3'C, 3'"C along with C7 appears at the same position (δ = 124.69 ppm). The vinyl carbons i.e. 1"C (of *3, 4 structure*) and 4'"C (of *1, 2 vinyl*) appeared as a single peak at 107.1 ppm. As in ^{1}H NMR, the two methyl carbons attached to the C8 centre for all the microstructures were detected at up-field values (δ = 25.8 and 17.7 ppm). Due to the presence of attached hydrogen with 3" C, it showed an upfield value (δ = 39.9 ppm) compared to 2'"C (δ = 40.37 ppm). Due to *–cis* structure, 5C is least shielded followed by 5"C. The close proximity of the polymer chains with 5'C and 5'"C leads to the higher shielding effect which reduces the chemical shift values. All other methylene protons (1, 4 and 6 Cs) appear in the range of 29.7 – 26.5 ppm and are overlapped with each other.

^{1}H NMR data of PMy$_{redox}$ ($CDCl_3$, 400 MHz, δ ppm): 5.14 [3, 7, 3', 7' H]; 2.02 [1, 4, 5, 6, 1', 4', 5', 6' H]; 1.64 [10, 10' H]; 1.27 [9, 9' H].

As shown in Fig. 3d, the ^{1}H NMR spectrum of redox initiated polymyrcene shows a single peak at 5.14 ppm corresponding to olefinic protons (3, 7, 3', 7' H) of =CH- units. The absence of any other peak in the range of 4.5 to 5.5 ppm indicates that neither *3, 4 structure* nor *1, 2 vinyl* structure has formed and the microstructure predominantly contains *1, 4* addition product (mixture of *1, 4 –cis* and *1, 4 –trans*). No distinct peak for all other methylene and methyl protons is observed, rather a bimodal peak (δ = 2.02 ppm and 1.64 ppm) followed by a hump (δ = 1.27 ppm) is obtained in the ^{1}H NMR spectrum.

^{13}C NMR data of PMy$_{redox}$ ($CDCl_3$, 400 MHz, δ ppm): 139.01 [2, 2' C]; 131.41 [8, 8' C]; 124.43 [3, 7, 3', 7' C]; 37.09 [5, 5' C]; 30.42 [1 C]; 29.65 [1'C]; 26.97 [4, 6, 4', 6' C]; 25.70 [10, 10' C]; 17.70 [9, 9' C].

The ^{13}C spectrum (Fig. 3e) of redox initiated polymyrcene also does not contain the signature peak of 2" C (of *3, 4 structure*) and 1", 4'" C (of *3, 4 structure* and *1, 2 vinyl* structure respectively), indicating that the microstructure is devoid of *3, 4* and *1, 2 vinyl* defects. Due to lower reaction temperature, the side reactions are suppressed in the case of redox polymerisation, thereby leading to polymyrcene that is rich in *1, 4* microstructure. The chemical shift values of all the other methylene and methyl carbons are well in accordance with those of persulfate initiated polymyrcene.

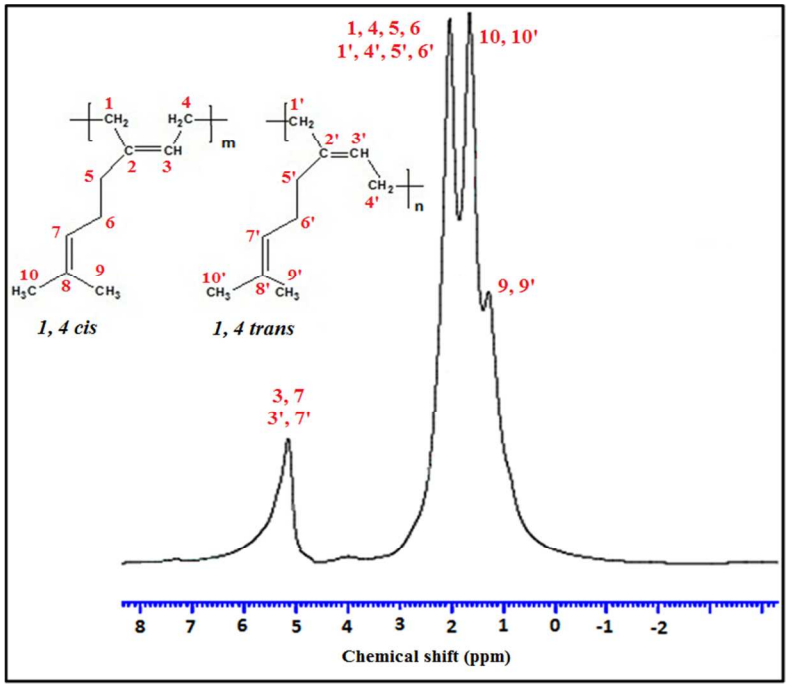

Fig. 3d: ^{1}H NMR spectrum of PMy_{redox}

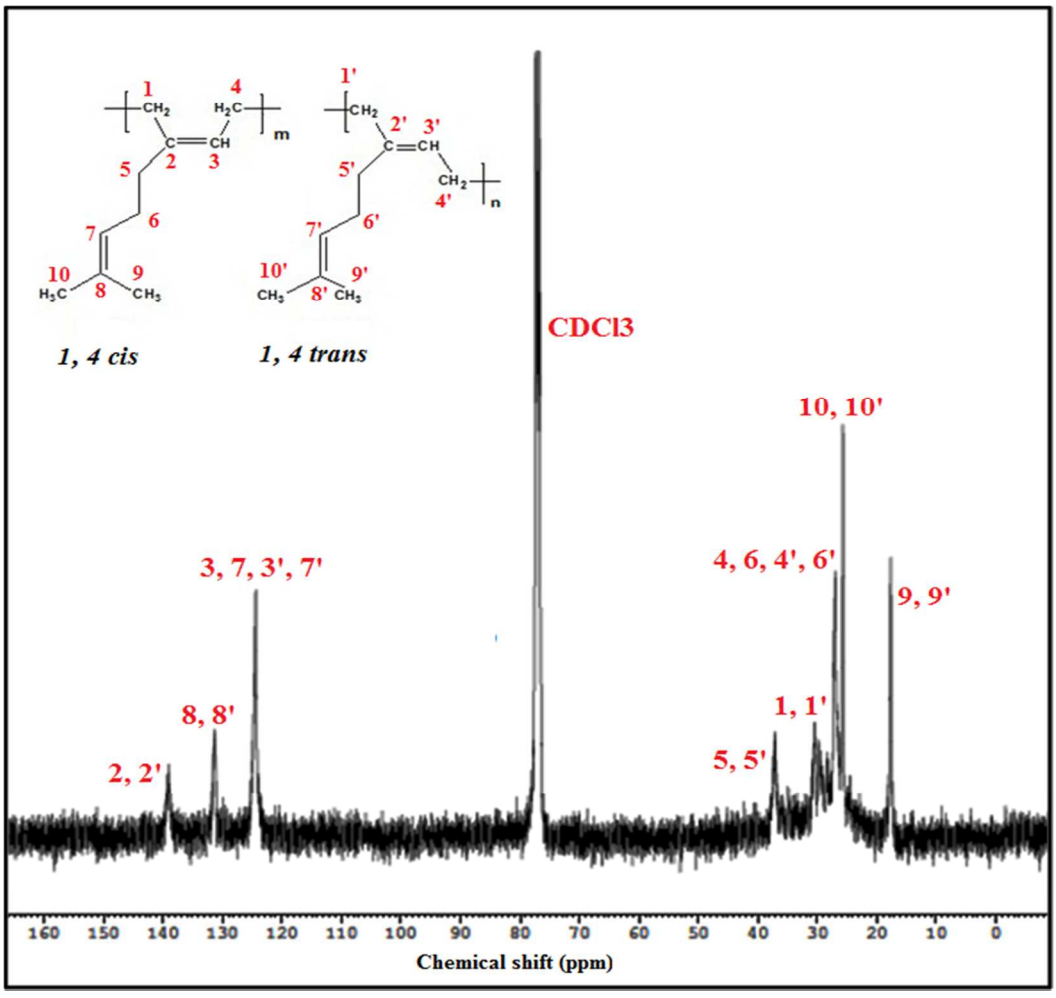

Fig. 3e: ^{13}C NMR spectrum of PMy_{redox}

Raman spectra of synthesised PMy

Raman spectra of β-myrcene and its polymer were recorded to compliment the observation of FTIR measurement. These are represented in Fig. 4. Raman band at 3006 cm^{-1} is assigned to the aliphatic =C-H stretching mode of C1, C3 and C4 centre which gets diminished after polymerisation. The combined $–CH_2$ and $–CH_3$ asymmetric stretching bands appear as a broad band at 2913 cm^{-1} in the spectrum of the monomer which are intensified after polymerisation. Raman bands at 1632 and 1670 cm^{-1} in the monomer are ascribed to the presence of conjugated (C1=C2 and C3=C4) and isolated (C7=C8) unsaturation respectively. It is anticipated that after polymerisation, the newly formed unsaturation (C2=C3) and the isolated one (C7=C8 as present in the monomer) appear as a single peak around 1668 cm^{-1}. A broad band around 1435 cm^{-1} in the monomer is assigned for $–CH_2$ bending which shifts to higher wave number value of 1444 cm^{-1} after polymerisation due to the formation of more such units, whereas the peak position due to $–CH_3$ bending at 1381 cm^{-1} remains unaltered even after polymerisation (though its intensity gets enhanced probably due to macromolecular entanglement after polymerisation). The peaks at 1287 and 1327 cm^{-1} in the polymer are due to the wagging vibration of the methylene unit.

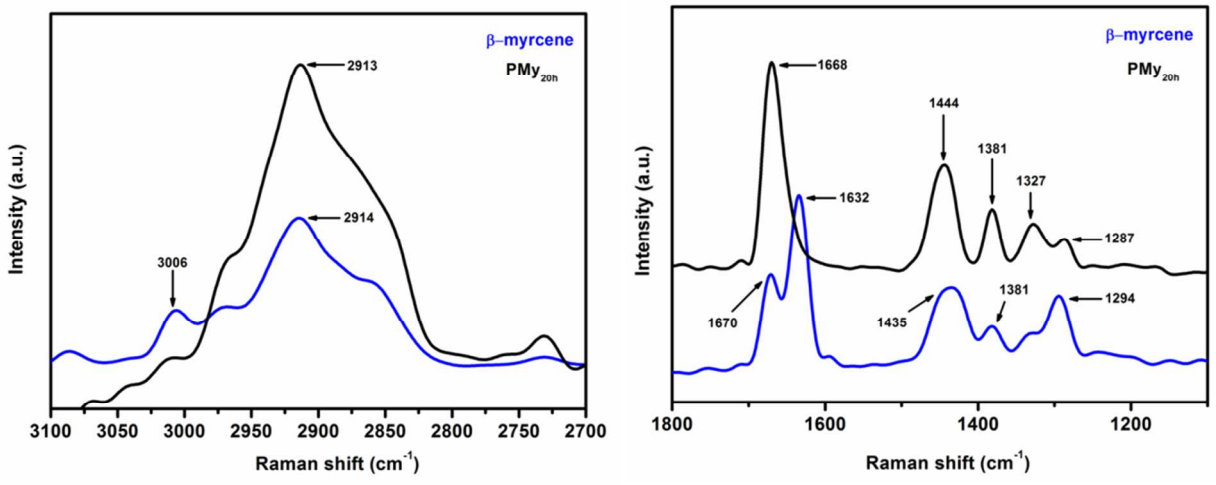

Fig. 4: Raman spectra of β-myrcene and PMy_{20h}

Theoretical studies

In order to understand the relation between chemical structure and reactivity, and to provide an insight into the electronic properties, Density Functional Theory (DFT) [34] calculation was performed with Becke's three-parameter hybrid functional (B3LYP) method using 6-311G (d, p) as a basis set. Calculations of molecular geometries and energy levels of polymers employing DFT is difficult due to their inherent macromolecular nature, but the calculation can be approximated using repeat unit of the same. [35] Fig. 5a represents the optimised structure of β-myrcene molecule in the ground state computed by B3LYP/6-311G (d, p) level. The frontier orbitals of the same are also presented in Fig 5b. It can be seen that though the HOMO is spread over the entire molecule, the LUMO is mainly localised onto the conjugated double bonds, i.e. C1=C2 and C3=C4 positions. Based on the B3LYP/6-311G (d, p) calculation, the energy of HOMO

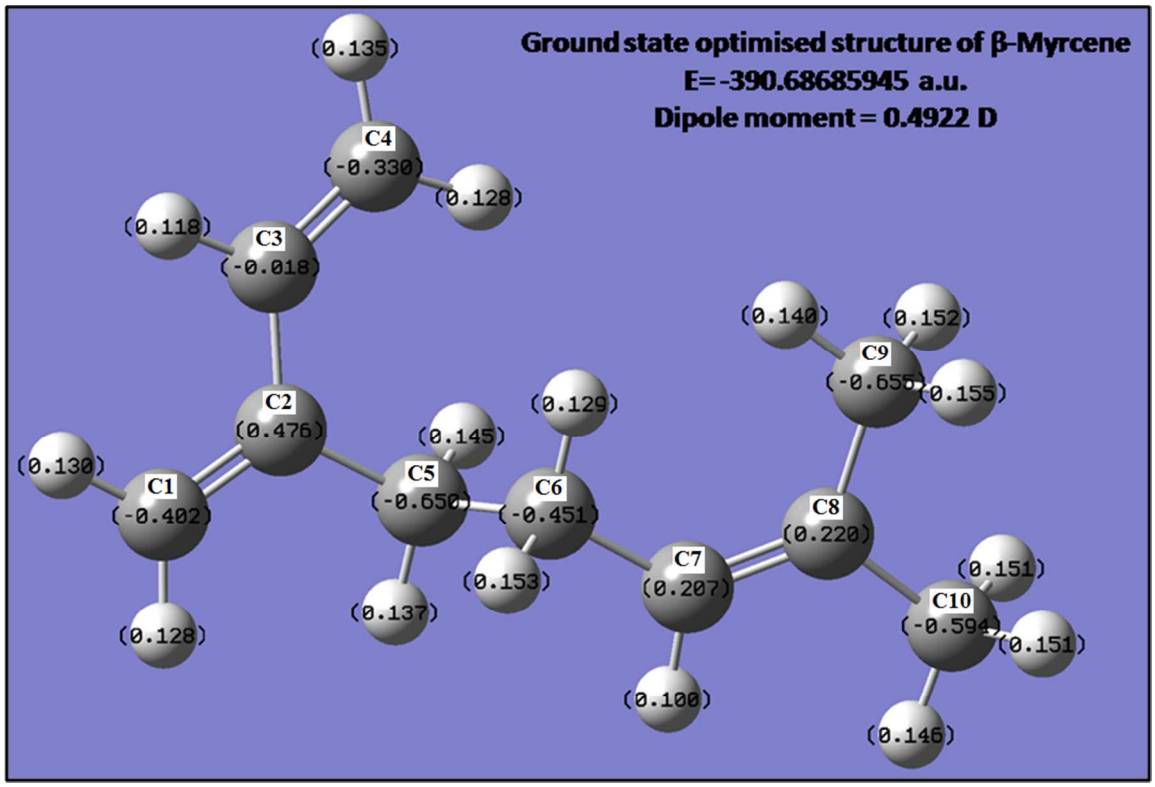

Fig. 5a: The ground state optimized structure of β-myrcene in B3LYP/6-311G (d, p).

and LUMO is found to be -6.355 and -1.078 eV respectively, thereby indicating possible charge transfer from HOMO to LUMO and subsequent accumulation of charges on the conjugated double bond makes it very much avid towards polymerisation. The value of ground state dipole moment of β-myrcene calculated by B3LYP/6-311G (d, p) level is 0.4922 Debye. To envisage the charge distribution three dimensionally, electrostatic potential mapping (ESP) of the β-myrcene monomer was done. It can be used to evaluate the electronic

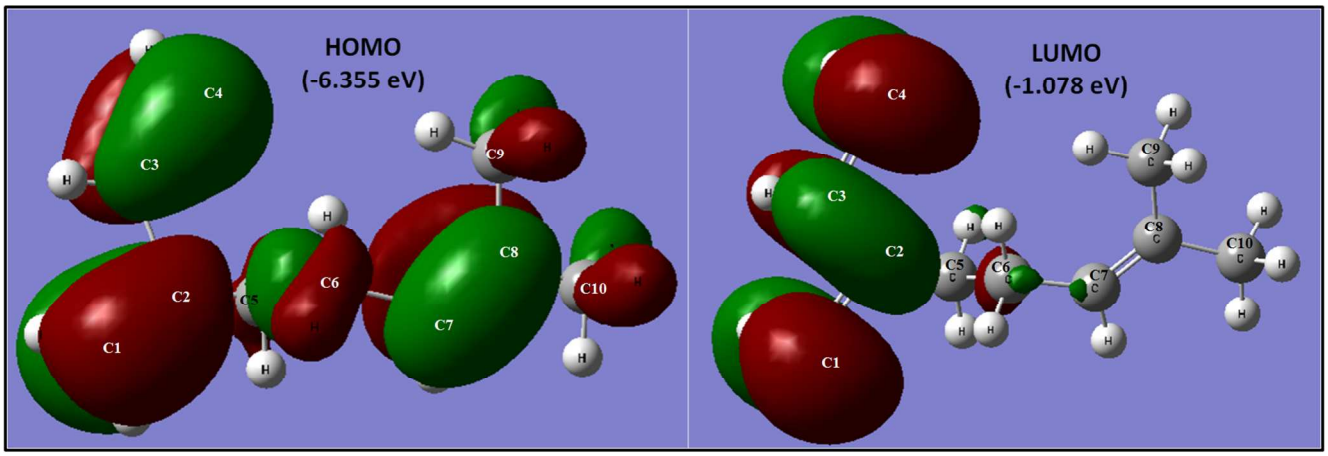

Fig. 5b: The molecular orbitals and their energies of β-myrcene molecule in the ground state in B3LYP/6-311G (d, p).

distribution around the molecular surface and has been used [35] for predicting sites and relative reactivity towards electrophilic attack. From the ESP mapping, it is clear that C1, C2, C3, C4 are surrounded by a greater density of negative charge, thus making this site potentially more prone towards polymerisation. Thus, combining the spectroscopic analysis and theoretical studies, it is evident that the polymerisation of β-myrcene proceeds via C1=C2 and C3=C4 pathways and the isolated unsaturation (C7=C8) remains unaltered.

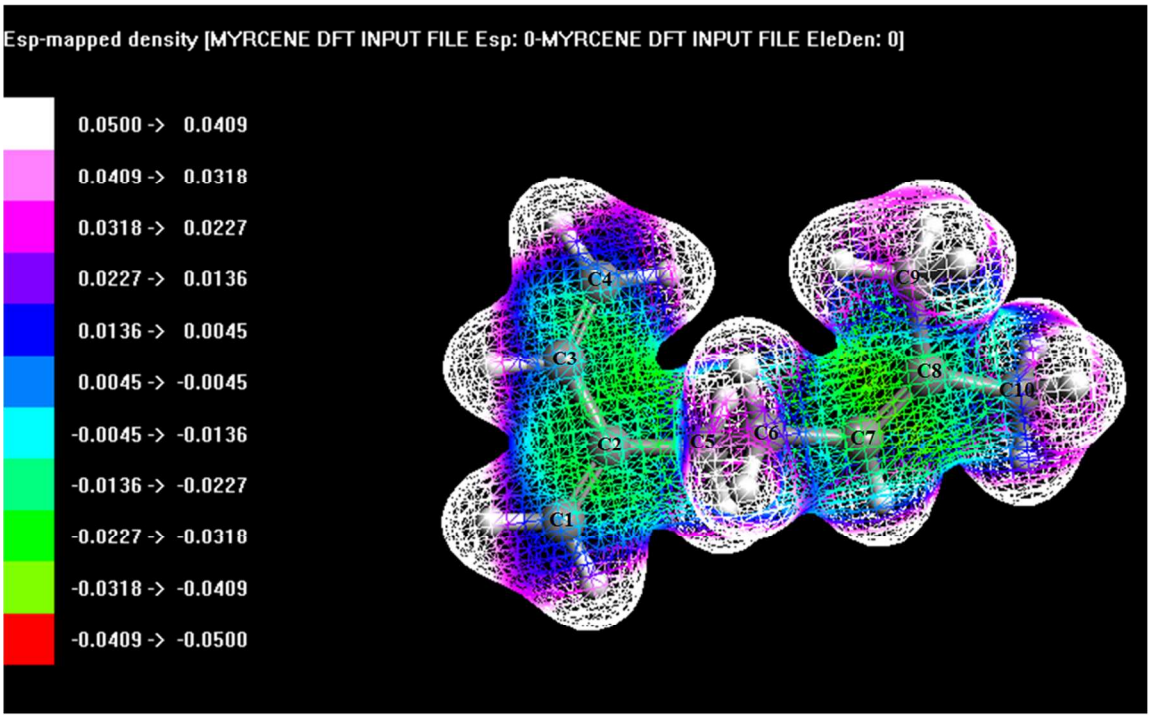

Fig. 5c: Electrostatic potential map for optimised β-myrcene molecule, high electrostatic potential: relative absence of electron; low electrostatic potential: relative abundance of electron.

Wide angle X-ray diffraction analysis of the synthesised PMy

X-ray diffraction analysis was performed to study the crystalline nature of the synthesised polymyrcene. The XRD plot (Fig. S1) of the synthesised polymer shows a broad hump at $2\theta = 19°$. Thus, the polymer film displayed a typical pattern of an amorphous polymer, much like a natural rubber. Branching at 2, 2', 3", 2"' C position in all of the microstructures prevents close packing of the chains, thereby rendering the polymer amorphous.

Thermal analysis of the synthesised polymer

Glass transition temperature (T_g) of a polymer plays an important role in dictating whether a particular polymer is in the rubbery state at room temperature. Elastomers are amorphous in nature and thus should have a T_g much below the ambient temperature, preferably at sub-zero range. Fig. 6a shows the DSC thermograms of persulfate and redox initiated polymer. For persulfate initiated polymyrcene, the DSC thermogram of second heating run shows a distinct baseline shift at around -73 °C which corresponds to the glass transition

temperature of the polymer. The transition temperature value is close to that of the natural rubber reported in literature, [36] thereby implying rubber like behaviour of the synthesised polymer. The redox variety of the polymer showed inflexion point at -60 °C, approximately 13 °C higher than the persulfate initiated species. This shift of temperature to higher value can be attributed to both increase in molecular weight which increases entanglement, thereby restricting segmental mobility, higher gel content and *1, 4* addition rich microstructure which facilitates dense packing compared to its persulfate initiated analogue. Fig. 6b represents the thermal decomposition curve of both persulfate and redox initiated polymyrcene. Unlike natural rubber, which shows a single degradation peak,

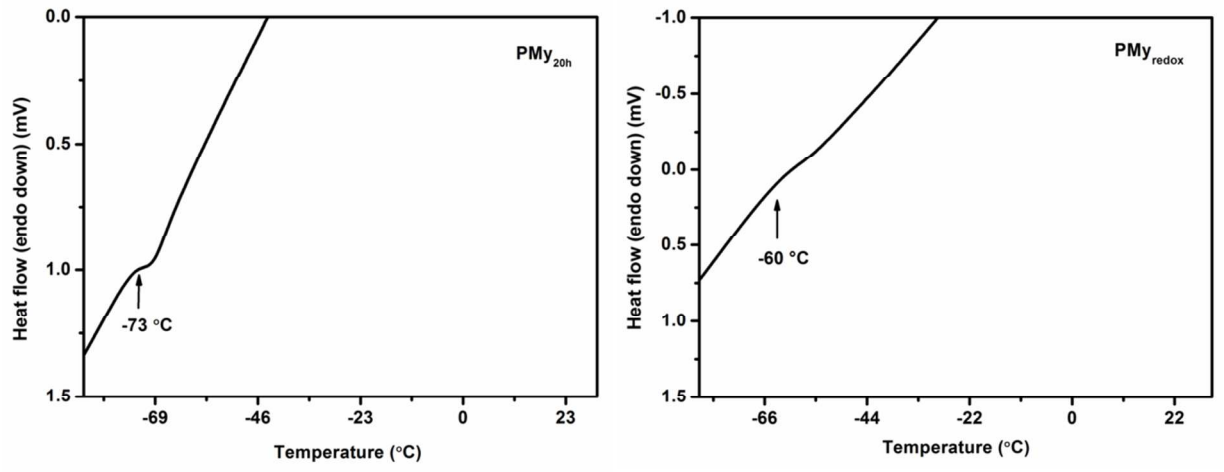

Fig. 6a: DSC thermograms of persulfate and redox initiated polymyrcene

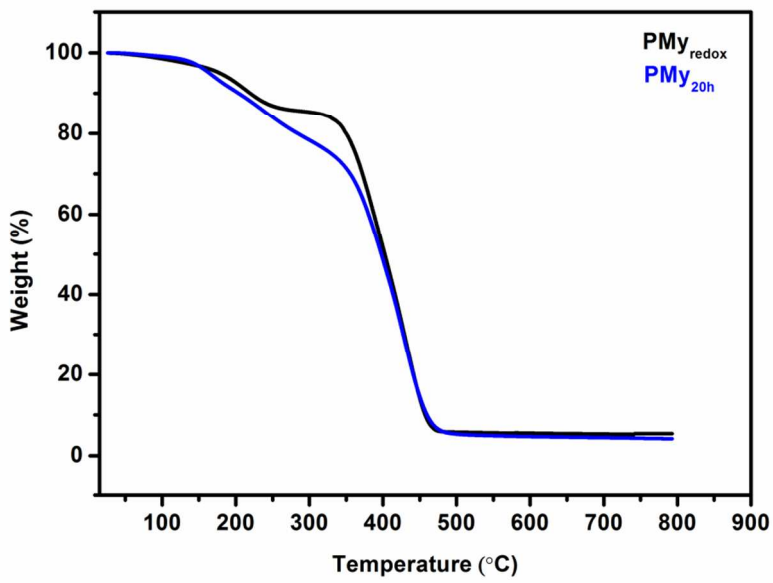

Fig. 6b: TGA thermograms of persulfate and redox initiated polymyrcene

the synthesised polymer exhibits two step degradation pattern. In the case of persulfate initiated polymyrcene, the sample weight gradually falls after onset of degradation, until it reaches ~ 425 °C beyond which the polymer degrades off quickly. In the case of redox initiated polymer, it shows a plateau after first weight loss and falls off rapidly upon reaching ~ 427 °C. As analysed from the NMR

spectra, the persulfate initiated polymyrcene contains *3, 4* and *1, 2 vinyl* defects in its microstructure in comparison to redox initiated polymyrcene which contains only *1, 4* microstructure. The effect of microstructure on the degradation of polybutadiene rubber is documented in the literature. [37]

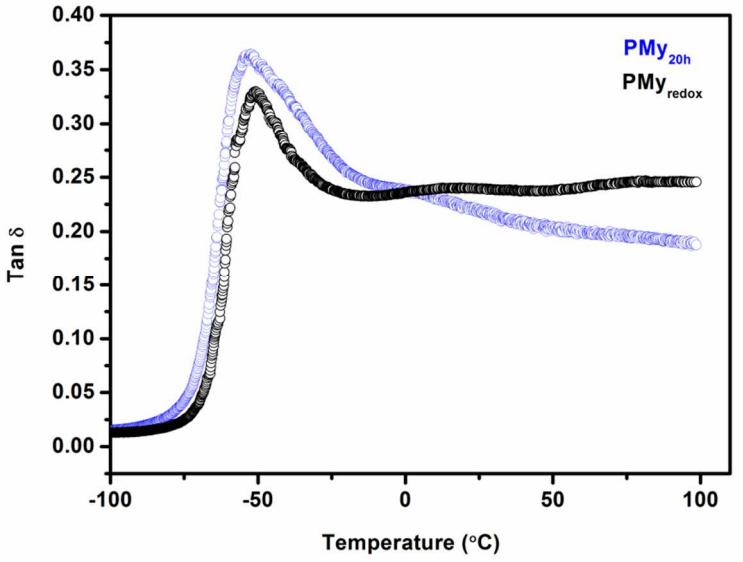

Fig. 7a: Tan δ overlay plot for persulfate and redox polymyrcene

Rheological studies and mechanical properties of the synthesised polymer

The tan δ versus temperature plot for both persulfate and redox polymyrcene are presented in Fig. 7a. The tan δ peak and hence the glass transition temperature of the persulfate and redox polymyrcene was found to be around -53.3 and -50.0 °C respectively. The numerical values follow the same trend as in DSC analysis. The higher T_g's are due to dynamic heating rate in the experiment. The monotonous decrease of complex viscosity with increasing angular frequency for both the samples is evident from Fig. 7b. It is anticipated that due to high molecular weight and defect free microstructure (*1, 4* microstructure aids in much dense packing) the complex viscosity for redox polymyrcene shows such higher value.

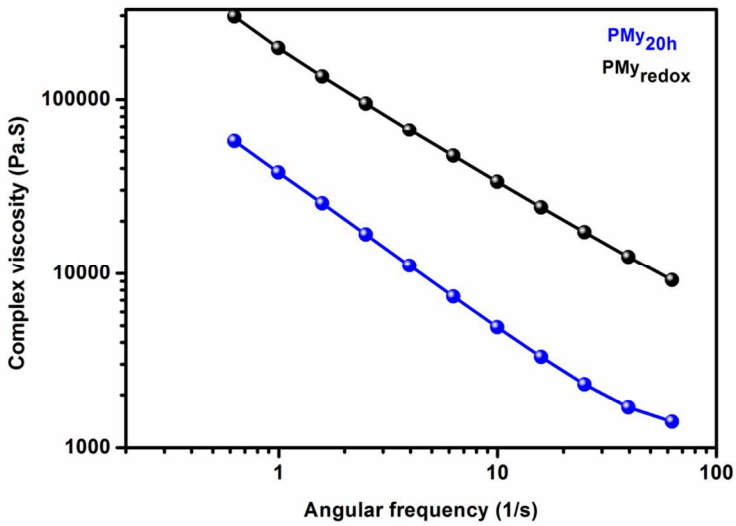

Fig. 7b: Plot of complex viscosity versus angular frequency for persulfate and redox polymyrcene

In order to understand the flow behaviour of the synthesised polymer, Power Law model [38] was employed. Power Law relates complex viscosity (η*) with angular frequency (ω) by flow consistency index (k) and flow behaviour index (n) by the following equation:

$$\eta * = k\omega^{(n-1)} \quad \text{.....(1)}$$

After linear curve fitting, from the slope, flow behaviour index for both the polymers was found to be less than one (n<1), indicating pseudoplastic nature (shear thinning behaviour). [38] PMy_{redox}, having higher 'n', is less shear thinning than PMy_{20h}. The tan δ value at 0 °C (indirect measure of wet skid resistance) and 60 °C (indirect measure of rolling resistance) for the synthesised polymer are presented in Table 4.

Table 4: Rheological analysis of synthesised polymyrcene

Sample	# T_g (°C)	*Tan δ at 0 °C	*Tan δ at 60°C	*Flow behaviour index (n)
PMy_{20h}	-53.3	0.238	0.199	0.167 *(R^2 = 0.9948)*
PMy_{redox}	-50.0	0.236	0.240	0.250 *(R^2 = 0.9988)*

#Data presented from dynamic mechanical analyser

**Data presented from modular compact rheometer*

The tensile stress-strain plot of the synthesised polymer is presented in Fig. 7c. The strips were prepared by casting a solution of synthesised polymer in chloroform on Teflon® petri-dish and driving off the solvent at room temperature. The stress-strain curve for persulfate initiated polymyrcene (unvulcanised and gum) shows higher tensile strength value (97.8 kPa) and higher elongation (upto 60 %) than the redox polymyrcene. It is anticipated that presence of *3, 4* and *1, 2 vinyl* microstructure leads to higher physical entanglement in the case of persulfate polymyrcene which aids in higher elongation and tensile strength. The relatively high *1, 4 –trans* content in redox polymyrcene hinders such phenomenon. Table 5 presents the mechanical properties of the polymyrcene polymers. These values are similar to other unvulcanised and gum rubbers. [39] Hence, this elastomer may find application as a single rubber, in polymer blends, composites as well as in adhesives.

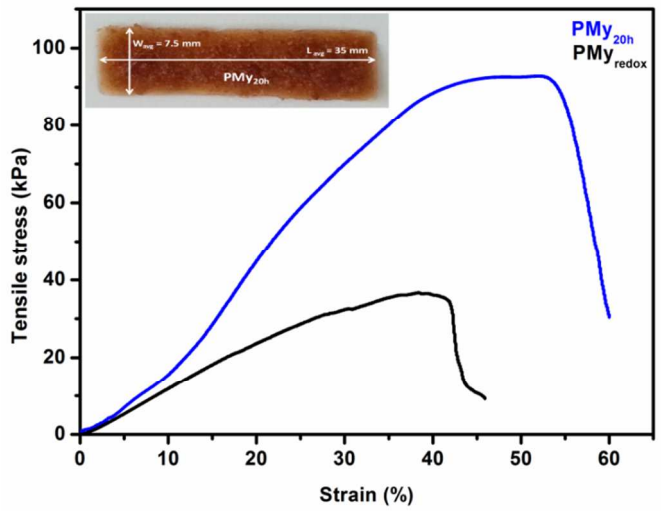

Fig. 7c: Tensile stress-strain plot of synthesised polymyrcene (inset shows a representative strip of polymyrcene used in tensile measurements)

Table 5: Mechanical properties of the synthesised polymyrcene

Sample	Modulus @ 20% (kPa)	Ultimate stress (kPa)	Breaking stress (kPa)	EAB (%)
PMy_{20h}	2.22 (± 0.05) [#]	97.8 (± 0.7)	42.2 (± 0.5)	60 (± 2)
PMy_{redox}	1.18 (± 0.01)	36.7 (± 0. 6)	8.9 (± 0.4)	46 (± 1)

[#] *Values in the parenthesis indicate the standard deviation based on three measurements.*

Analysis of particle morphology of the latex emulsion

To analyse the particle nature of the latex, dynamic light scattering method was used and the particle nature of the latex was further confirmed from FESEM images. The particle size distribution and mean particle size of the polymyrcene latex taken at different time intervals are presented in Fig. S2. The particle size increases from 52.6 nm at 4h to 72.1 nm at 24h at 70 °C. The FESEM images (Fig. S3) were taken by drop casting the latex emulsion on silicon wafer and subsequently driving off the water. Due to the removal of the dispersion medium, the particles tend to coalesce with each other, thereby becoming prone to form larger aggregates (black circles in Fig. S3). However, we measured the diameter of the nodules in the aggregates. The average diameter is in accord with the value obtained from DLS measurements.

Conclusions

In the present work, we have successfully synthesised a bio-based elastomer from naturally occurring monoterpene, β-myrcene, utilising emulsion polymerisation technique. The polymyrcene synthesised following the optimised set of reaction conditions (at 70 °C for 20h) displayed reasonably high molecular weight of 92,860 Da and a subzero glass transition temperature of -73 °C. From the ^{1}H and ^{13}C NMR analysis, it was found that the persulfate initiated polymyrcene contained *1, 2 vinyl* and *3, 4* defects along with *1, 4 cis* and *1, 4 trans* microstructure. The redox analogue showed number average molecular weight of 1,09,780 Da. The absence of peak in the range of δ = 4.5 to 5.5 ppm in the ^{1}H NMR spectrum indicated that it contained predominately *1, 4* microstructures. Spectroscopic measurements coupled with DFT calculation confirmed the participation of conjugated double bond in the polymerisation process and simultaneous conservation of the isolated one. The complex viscosity data was fitted to Power Law model and the finding revealed the pseudoplastic behaviour of the synthesised polymer. The amorphous nature, glass transition temperature and thermal stability of the synthesised polymyrcene were found to be similar to those of other rubbers, thus paving the way for its application as an elastomer of the future.

Acknowledgement

Part of the work and analysis of the results were carried out at Indian Institute of Technology Kharagpur. PS would like to acknowledge the facilities provided by IIT Kharagpur.

References:

[1] Gandini A., Polymers from Renewable Resources: A Challenge for the Future of Macromolecular Materials, *Macromolecules*, 2008, **41**, 9491.

[2] Singh R., Facts, Growth and Opportunities in Industrial Biotechnology, *Organic Process Research & Development*, 2010, **15**, 175.

[3] Yang J., Zhao G., Sun Y., Zheng Y., Jiang X., Liu W., Xian M., Bio-isoprene Production Using Exogenous MVA Pathway and Isoprene Synthase in Escherichia coli, *Bioresource Technology*, 2012, **104**, 642.

[4] Bhowmick A. K., Stephens H. L., *Handbook of Elastomers*, Marcel Dekker AG, New York, 2001, Ch 2.

[5] Belgacem M. N., Gandini A., *Monomers, Polymers and Composites from Renewable Resources,* Elsevier, Amsterdam, 2008, Ch 2.

[6] Erman W. F., *Chemistry of Monoterpenes*, Marcel Dekker, New York, 1985.

[7] Finar I. L., *Organic Chemistry Vol. 2, Stereochemistry and The Chemistry of Natural Products*, Longmans Green and Co. Ltd., London, 1964, Ch 8.

[8] Wilbon P. A., Chu F., Tang C., Progress in Renewable Polymers from Natural Terpenes, Terpenoids and Rosin, *Macromolecular Rapid Communication*, 2013, **34**, 8.

[9] Firdaus M., de Espinosa Lucas M., Meier Michael A. R., Terpene-Based Renewable Monomers and Polymers via Thiol-Ene Additions, *Macromolecules*, 2011, **44**, 7253.

[10] Corma A., Iborra S., Velty A., Chemical Routes for the Transformation of Biomass into Chemicals, *Chemical Reviews*, 2007, **107**, 2411.

[11] Grau E., Mecking S., Polyterpenes by Ring Opening Metathesis Polymerization of Caryophyllene and Humulene*, RSC Green Chemistry*, 2013, **15**, 1112.

[12] Sharma S., Srivastava A. K., Synthesis and Characterization of Copolymers of Limonene with Styrene Initiated by Azobisisobutyronitrile*, European Polymer Journal*, 2004, **40,** 2235.

[13] Firdaus M., Meier Michael A. R., Renewable Polyamides and Polyurethanes Derived from Limonene, *RSC Green Chemistry*, 2013, **15**, 370.

[14] Puskas J. E., Gergely A. L, Kaszas G., Controlled/Living Carbocationic Copolymerization of Isobutylene with Alloocimene, *Journal of Polymer Science Part A: Polymer Chemistry*, 2013, **51**, 29.

[15] Shi Y., Shan G., Shang Y., Role of Poly(ethylene glycol) in Surfactant-free Emulsion Polymerization of Styrene and Methyl methacrylate*, Langmuir*, 2013, **29**, 3024.

[16] Satoh K., Sugiyama H., Kamigaito M., Biomass Derived Heat Resistant Alicyclic Hydrocarbon Polymers: Poly(terpenes) and Their Hydrogenated Derivatives, *RSC Green Chemistry*, 2006, **8**, 878.

[17] Kukhta N. A., Vasilenko I. V., Kostjuk S. V., Room Temperature Cationic Polymerization of β-pinene Using Modified $AlCl_3$ Catalyst: Toward Sustainable Plastics From Renewable Biomass Resources*, RSC Green Chemistry*, 2011, **13**, 2362.

[18] Matsuda M., Satoh K., Kamigaito M., 1:2-Sequence-Regulated Radical Copolymerization of Naturally Occurring Terpenes with Maleimide Derivatives in Fluorinated Alcohol, *Journal of Polymer Science Part A: Polymer Chemistry*, 2013, **51**, 1774.

[19] Alvès M. H., Sfeir H., Tranchant Jean F., Gombart E., Sagorin G., Caillol S., Billon L., Save M., Terpene and Dextran Renewable Resources for the Synthesis of Amphiphilic Biopolymers, *Biomacromolecules*, 2014, **15**, 242.

[20] Behr A., Johnen L., Myrcene as a Natural Base Chemical in Sustainable Chemistry: A Critical Review, *ChemSusChem*, 2009, **2**, 1072.

[21] Tracy N. I., Chen D., Crunkleton D. W., Price G. L., Hydrogenated Monoterpenes as Diesel Fuel Additives, *Fuel*, 2009, **88**, 2238.

[22] Kobayashi S., Lu C., Hoye Thomas R., Hillmyer Marc A., Controlled Polymerization of a Cyclic Diene Prepared from the Ring-Closing Metathesis of a Naturally Occurring Monoterpene*, Journal of American Chemical Society*, 2009, **131**, 7960.

[23] Loughmari S., Hafid A., Bouazza A., Bouadili Abdelaziz E., Zinck P., Visseaux M., Highly Stereoselective Coordination Polymerization of β-Myrcene from a Lanthanide-Based Catalyst: Access to Bio-Sourced Elastomers, *Journal of Polymer Science Part A: Polymer Chemistry*, 2012, **50**, 2898.

[24] Marval C. S., Hwa Charles C. L., Polymyrcene, *Journal of Polymer Science*, 1960, **XLV**, 25.

[25] Choi S. W., Ritter H., Novel Polymerization of Myrcene in Aqueous Media via Cyclodextrin-Complexes, *e-Polymers*, 2007, **45**, 1.

[26] van Herk A., *Chemistry and Technology of Emulsion Polymerisation*, Blackwell Publishing, India, 2005.

[27] Wang R., Ma J., Zhou X., Wang Z., Kang H., Zhang L., Hua K. C., Kulig J., Design and Preparation of a Novel Cross-Linkable, High Molecular Weight and Bio-Based Elastomer by Emulsion Polymerization, *Macromolecules*, 2012, **45**, 6830.

[28] Johanson A. J., McKennon F. L., Goldblatt F. L., Emulsion Polymerisation of Myrcene, Industrial and Engineering Chemistry, 1948, **40**, 500.

[29] Kumar K. Dinesh, Gupta S., Sharma B. B., Tsou Andy H., Bhowmick A. K., Probing the Viscoelastic Properties of Brominated Isobutylene-co-p-Methylstyrene Rubber/Tackifier Blends Using a Rubber Process Analyzer*, Polymer Engineering and Science*, 2008, **48**, 2400.

[30] Gergely A. L., Ph.D. Thesis, University of Akron, 2014.

[31] Newmark R., Majumdar R., ^{13}C-NMR Spectra of cis-Polymyrcene and cis-Polyfarnesene, *Journal of Polymer Science Part A: Polymer Chemistry*, 1988, **26**, 71.

[32] Stoffelbach F., Tibiletti L., Rieger J., Charleux B., Surfactant-Free, Controlled/Living Radical Emulsion Polymerization in Batch Conditions Using a Low Molar Mass, Surface-Active Reversible Addition-Fragmentation Chain-Transfer (RAFT) Agent, *Macromolecules*, 2008, **41**, 7850.

[33] Kostjuk S. V., Ouardad S., Peruch F., Deffieux A., Absalon C., Puskas J. E., Ganachaud F., Carbocationic Polymerization of Isoprene Co-initiated by $B(C_6F_5)_3$: An Alternative Route Toward Natural Rubber Polymer Analogues?, *Macromolecules*, 2011, **44**, 1372.

[34] Frisch M. J., Trucks G. W., Schlegel H. B., Scuseria G. E., Robb M. A., Cheeseman J. R., Scalmani G., Barone V., Mennucci B., Petersson G. A., Nakatsuji H., Caricato M., Li X., Hratchian H. P., Izmaylov A. F., Bloino J., Zheng G., Sonnenberg J. L., Hada M., Ehara M., Toyota K., Fukuda R., Hasegawa J., Ishida M., Nakajima T., Honda Y., Kitao O., Nakai H., Vreven T., Montgomery J. A., Peralta J. E., Ogliaro F., Bearpark M., Heyd J. J., Brothers E., Kudin K. N., Staroverov V. N., Keith T., Kobayashi R., Normand J., Raghavachari K., Rendell A., Burant J. C., Iyengar S. S., Tomasi J., Cossi M., Rega N., Millam J. M., Klene M., Knox J. E., Cross J. B.,

Bakken V., Adamo C., Jaramillo J., Gomperts R., Stratmann R. E., O. Yazyev, A. J. Austin, R. Cammi, C. Pomelli, J. W. Ochterski, Martin R. L., Morokuma K., Zakrzewski V. G., Voth G. A., Salvador P., Dannenberg J. J., Dapprich S., Daniels A. D., Farkas O., Foresman J. B., Ortiz J. V., Cioslowski J., Fox D. J., *Gaussian 09*, Revision, Gaussian Inc., Wallingford, CT, 2010.

[35] Gula A., Akhterb Z., Qureshib R., Bhattia Arshad S., Conducting Poly(azomethine)ester: Synthesis, Characterization and Insight into electronic properties using DFT calculations*, RSC Advances*, 2014, **4**, 22094.

[36] Roland C. Michael, Glass Transition in Rubbery Materials, *ACS Rubber Chemistry and Technology*, 2012, **85**, 313.

[37] Luda M. P., Guaita M., Chiantore O., Thermal Drgradation of Polybutadiene, 2 Overall Thermal Behaviour of Polymers with Different Microstructure, *Macromolecular Chemistry and Physics*, 1992, **193**, 113

[38] Sadhu S., Bhowmick A. K., Unique Rheological Behaviour of Rubber Based Nanocomposites, *Journal of Polymer Science: Part B, Polymer Physics,* 2005, **43**, 1854.

[39] Bhowmick A. K., De P. P., Bhattacharyya A. K., Adhesive Tack and Green Strength of EPDM Rubber, *Polymer Engineering and Science*, 1987, **27**, 1195.